ELSEVIER

Chemical Engineering Journal 122 (2006) 47–53

Chemical Engineering Journal

www.elsevier.com/locate/cej

On the influence of sodium chloride concentration on equilibrium contact angle

N. Sghaier, M. Prat *, S. Ben Nasrallah

Laboratoire d'Etudes des Systèmes Thermiques et Energétiques, Ecole Nationale d'Ingénieurs de Monastir, Monastir 5000, Tunisia

Received 12 July 2005; received in revised form 28 November 2005; accepted 24 February 2006

Abstract

We report experimental results on the influence of sodium chloride concentration on the equilibrium contact angle of droplets of NaCl–water in the presence of air on various surfaces, including hydrophilic and hydrophobic glass plates, Plexiglas, RTV and silicon. It is found that the contact angle significantly increases with NaCl concentration on all hydrophilic surfaces. The contact angle variations are small on the tested hydrophobic surfaces. A simple expression deduced from the Young relation is proposed as a rough estimate of the variations of contact angle with salt concentration. These results are discussed in relation with various salt related transport problems in porous media, such as evaporation, salt weathering and soil contamination.

Keywords: Salt transport; Contact angle; Wettability; Porous media

1. Introduction

The motivation for the present study stems from several environmental problems involving salt transport in unsaturated porous media such as the salt weathering problem or the soil salinisation problem. The salt weathering problem refers to the deterioration of building materials resulting from the crystallisation of salt in the pores, e.g. [1]. In this context, crystallisation induces by evaporation is a widely accepted process of salt crystal formation. When the water partially saturating the pore space of a porous material evaporates, the concentration of salt dissolved into the water contained in the pores increases. When the salt concentration becomes high enough, salts crystallise and can induce damages due to stresses on the pore walls generated by the crystal growth. The soil salinisation problem refers to the degradation of soils due to high levels of salt, e.g. [2]. Plants and soil organisms can be killed or their productivity severely limited on affected lands. For both problems a good understanding of water and ions transport in unsaturated porous medium is needed.

The theory for modelling these transport phenomena is relatively well established, at least before crystallisation occurs, e.g. [3–6] and references therein. In most of the models, the porous medium is a continuum: the dependent variables, like saturation, are volume-averaged quantities and the relation of fluxes to gradients is through semi-empirical coefficients such as relative permeabilities or effective diffusion coefficient. Capillary effects are taken into account through the concept of macroscopic capillary pressure. The macroscopic capillary pressure is a function of saturation and depends on surface tension and wetting properties of porous matrix. For simple systems such as a couple of two immiscible fluids in contact with a surface of well-defined mineral composition, the wettability of the system can be defined using the concept of equilibrium contact angle, e.g. [7], which is the angle θ between the solid phase and the interface between the two fluids (see Fig. 1). When the two fluids are liquid water and air, the surface is said to be hydrophilic when this angle is lower than 90° and hydrophobic when $\theta > 90°$. In a porous medium, it can be difficult to characterize the wettability by means of the contact angle because it cannot be measured within the porous medium. Also, the chemical composition of pore walls may vary, which can lead to variation in wettability within the pore space. Thus, although characterizing the wettability of a porous medium may be subtle, the transport phenomena in an unsaturated porous medium are strongly dependent on the wetting properties when capil-

* Corresponding author at: Institut de Mécanique de Fluide de Toulouse, UMR CNRS-INPT/UPS no 5502, Allée du professeur Camille Soula, Toulouse 31400, France. Tel.: +33 561 28 58 83; fax: +33 561 28 58 78.
E-mail address: prat@imft.fr (M. Prat).

1385-8947/$ – see front matter © 2006 Elsevier B.V. All rights reserved.
doi:10.1016/j.cej.2006.02.017

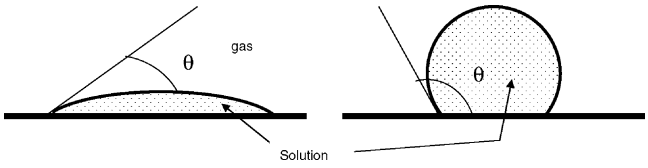

Fig. 1. Hydrophilic ($\theta < \pi/2$) and hydrophobic ($\theta > \pi/2$) surfaces.

lary effects are a dominant mechanism, which is generally the case in the problems mentioned before. The influence of wetting properties is still more explicit in the recent works focussing on pore-level studies, e.g. [8]. The contact angle is one of the key parameter of pore-network models.

Surprisingly, to the best of our knowledge, the study of the influence of salt concentration on the equilibrium contact angle has not been addressed except for the results reported in Ref. [9]. Their data indicate a small increase of the contact angle of NaCl–water solution on glass with the NaCl concentration. However, these data are limited to a narrow range of very small NaCl concentration. In this paper, we report experimental results on the influence of sodium chloride concentration on the equilibrium contact angle of droplets of NaCl–water in the presence of air on various surfaces, including hydrophilic and hydrophobic surfaces.

The paper is organized as follows. We present, first, the solid/liquid/gas systems that have been studied as well as useful information on experimental procedures. Then, we present the results of contact angle measurements as a function of salt concentration. Finally, the potential impact of the results on the physics of water movement and ion transports in an unsaturated porous medium is discussed.

2. Plate preparation and contact angles

2.1. Systems under study

We study systems formed by droplets of liquid on various surfaces in the presence of air. The liquid is a solution of distilled water and sodium chloride. The amount of NaCl in the solution is characterized by its mass fraction $C = \rho_s/(\rho_s + \rho_w)$, where ρ_s and ρ_w are the salt and water density in the solution, respectively. C varies in the range $[0, C_{sat}]$, where C_{sat} is the saturation concentration. For sodium chloride at 20 °C, $C_{sat} = 26.4$. The considered solid surfaces are hydrophilic glass, silanized glass, glass coated with Rhodorsil® RTV-2 (a silicone elastomer), Plexiglas, and silicon wafers. As we will see, silanized glass and glass coated with Rhodorsil® RTV-2 are hydrophobic. Plexiglas is slightly hydrophilic whereas the untreated glass and the silicon wafers are hydrophilic. The glass samples are either microscope cover glasses (referenced to as MCG in the tables below) or standard commercial glass (referenced to as CG).

2.2. Contact angle measurement technique

Equilibrium contact angle measurements were performed using GBX™ digidrop autogoniometers. The measurements were made in three different laboratories but with the same type of apparatus. In the tables summarizing the results, the three laboratories are identified as lab#1, lab#2 and lab#3, respectively. The measurements were made in a cleanroom in lab#3 whereas they were made in an ordinary room in the other labs. Measurements were made on sessile drops of distilled water for various NaCl concentrations by measuring the tangent to the drop at its intersection with the surface. Values obtained are the mean of the tangents taken at both sides of each droplet. For each NaCl concentration, measurements were made on drops placed at different locations on the plate surface. Details on the number of drops considered for each measurement are given in Section 3. A measurement takes about 10 s and is performed at the room temperature (≈20 °C). Hence, droplet evaporation is negligible over the measurement duration. The solid surfaces were cleaned with ethanol before each measurement or with sulfochromic acid (glass, lab#2) or with a H_2O_2–H_2SO_4 piranha solution (glass, lab#3). More precisely at lab#2, each glass plate was immersed 1 h in sulfochromic acid, and then rinsed two times with distilled water. At lab#3, each glass plate was rinsed with distilled water, and then dried under N_2 after immersion into the piranha solution.

2.3. Plate surface functionalization

Hydrophobic glass plates are obtained by silanization of the glass surface. This surface modification is accomplished by liquid phase deposition of silane in an organic solvent. There exist various procedures for performing the chemical bonding of silane monolayer at the surface, e.g. [9]. Two steps can be distinguished: cleaning and silanization. The procedure we use for each step can be summarized as follows. Plate cleaning procedure: rinse with trichloroethylene, dry under N_2, rinse with acetone, dry under N_2, rinse with ethanol, dry under N_2. Plate silanization procedure: immerse the plate 5 min in H_2O_2–H_2SO_4 piranha solution, rinse in H_2O, dry under N_2, dry in an oven 12 h at 150 °C, immerse 30 min the plate in a solution of trichloroethylene and OTS (octadecyltrichlorosilane), immerse 5 min the plate in trichloroethylene, rinse with trichloroethylene, dry under N_2.

We have also made an experiment with a glass plate coated with Rhodorsil® RTV-2 (a silicone elastomer). As shown below, RTV renders the plate still more hydrophobic than silanization.

3. Results

The contact angle measurement results are summarized in Tables 1–5. We begin with the hydrophilic surfaces. Fig. 2 shows the evolution of contact angle as a function of NaCl concentration for the hydrophilic glass samples. Clearly, the contact angle increases with the salt concentration, see also Table 1. The results with the microscope cover glass for series GPHI1 and GPHI2 are in a relatively good agreement and indicate an increase of several tens of percentage over the considered range of concentration. However, the data for series GPHI3 (which corresponds to microscope cover glass cleaned with the piranha solution) differ from the two other series (cleaned with ethanol or sulfochromic acid, respectively). A significant contact angle

Table 1
Equilibrium contact angle for the hydrophilic glass plate

C (%)	θ (°) (Eq. (2))	θ (°)	S.D. (°)	Number of measures	Type of glass	Laboratory	Series
0	39.8	39.8	1.2	11	MCG	1	GPHI1
2.2	40.3	40.9	0.7	11	MCG	1	GPHI1
4.4	40.9	44.6	0.6	11	MCG	1	GPHI1
6.6	41.5	44.7	0.6	11	MCG	1	GPHI1
8.8	42.2	45.1	0.4	11	MCG	1	GPHI1
17.6	44.7	46.9	0.4	11	MCG	1	GPHI1
22	46.1	48.3	0.3	11	MCG	1	GPHI1
24.2	46.7	52.2	1.1	11	MCG	1	GPHI1
26.4	47.5	55.1	1.1	11	MCG	1	GPHI1
0	39.3	39.3	1.4	12	MCG	2	GPHI2
2.2	39.9	39.5	2.6	11	MGG	2	GPHI2
4.4	40.5	48.7	2.2	11	MGG	2	GPHI2
6.6	41.1	45.3	1.7	10	MCG	2	GPHI2
8.8	41.7	49.9	1.5	10	MCG	2	GPHI2
17.6	44.3	52.9	3.8	16	MCG	2	GPHI2
22	45.7	59.5	5.1	11	MCG	2	GPHI2
24.2	46.4	58.0	3.1	11	MCG	2	GPHI2
26.4	47.1	61.0	2.3	11	MCG	2	GPHI2
0	25.0	25.0	2.4	20	MCG	3	GPHI3
3	26.4	28.3	2.5	20	MCG	3	GPHI3
6	27.8	29.0	2.5	20	MCG	3	GPHI3
9	29.2	28.5	2.1	11	MCG	3	GPHI3
12	30.6	29.6	1.7	10	MCG	3	GPHI3
15	32.0	29.0	1.0	10	MCG	3	GPHI3
18	33.3	30.6	1.7	10	MCG	3	GPHI3
21	34.7	33.1	1.9	11	MCG	3	GPHI3
24	36.1	35.2	1.5	11	MCG	3	GPHI3
26.4	37.2	36.0	1.8	14	MCG	3	GPHI3
0	47.9	47.9	3.1	6	CG	3	GPHI4
12.5	50.6	61.8	2.3	6	CG	3	GPHI4
25	53.6	76.4	1.3	6	CG	3	GPHI4

θ is the mean value over the indicated number of measures, S.D. is the standard deviation. C is the sodium chloride concentration. MCG, microscope cover glass; CG, commercial glass.

increase is still obtained. However, the range of variation of contact angle is significantly narrower than for the two other series. Although limited to three concentrations, the data for the commercial glass plates (series GPHI4) lead to the same tendency, i.e. the increase of contact angle with concentration. The variations of contact angle for this series are a little greater than for series GPHI1 and GPHI2 but remain on the same order of magnitude.

The data for the silicon wafer see Table 2, also show that the contact angle increases with concentration. The increase over the studied range of concentration is on the order of 10°.

The data for Plexiglas reported in Table 3 confirm that the contact angle tends to increase with the concentration when the surface is hydrophilic. However, the contact angle is high, near

Table 2
Equilibrium contact angle for silicon wafers

C (%)	θ (°) (Eq. (2))	θ (°)	S.D. (°)	Number of measures	Laboratory	Series
0	41.3	41.3	0.7	4	3	S1
7.8	43.3	45.6	0.4	5	3	S1
15.5	45.4	50.0	1.1	10	3	S1
20	46.7	51.0	1.0	10	3	S1
23	47.6	52.9	0.5	5	3	S1
26.4	48.7	56.1	1.0	6	3	S1
0	47.9	47.8	0.4	5	3	S2
7.6	49.4	48.5	0.2	4	3	S2
14.5	51.0	50.1	0.3	4	3	S2
17.7	51.7	52.4	0.3	4	3	S2
20.8	52.4	54.5	1.2	5	3	S2
23.7	53.2	55.3	1.7	2	3	S2
26.4	53.9	57.8	1.4	5	3	S2

θ is the mean value over the indicated number of measures, S.D. is the standard deviation. C is the sodium chloride concentration.

Table 3
Equilibrium contact angle for Plexiglas plate

C (%)	θ (°) (Eq. (2))	θ (°)	S.D. (°)	Number of measures	Laboratory	Series
0	81.2	81.2	5.0	9	1	P1
5	81.4	80.9	1.2	9	1	P1
12.5	81.7	84.3	1.2	9	1	P1
25	82.2	82.7	4	9	1	P1
0	72.6	72.6	10.0	6	2	P2
12	73.5	75.3	2.1	6	2	P2
26.4	74.8	85.8	3.4	6	2	P2
0	87.1	87.1	4.6	11	3	P3
12.5	87.3	84.1	1.7	6	3	P3
25	87.5	80.7	4.4	13	3	P3

θ is the mean value over the indicated number of measures, S.D. is the standard deviation. C is the sodium chloride concentration.

Table 4
Equilibrium contact angle for a silanized glass plate

C (%)	θ (°) (Eq. (2))	θ (°)	S.D. (°)	Number of measures	Type of glass	Laboratory
0	107.9	107.9	5.5	12	CG	1
5	107.5	100.6	1.3	12	CG	1
12.5	107.0	103.1	4.5	12	CG	1
25	105.8	107.2	6.9	12	CG	1

θ is the mean value over the indicated number of measures, S.D. is the standard deviation. C is the sodium chloride concentration.

Table 5
Equilibrium contact angle for RTV-2

C (%)	θ (°) (Eq. (2))	θ (°)	S.D. (°)	Number of measures	Laboratory
0	110.3	110.3	1.7	9	1
5	109.9	108.8	0.6	9	1
12.5	109.2	109.7	2.5	9	1
25	107.9	107.1	3.0	9	1

θ is the mean value over the indicated number of measures, S.D. is the standard deviation. C is the sodium chloride concentration.

80°, even for pure water and this tendency is less marked than for glass and silicon, especially for series P1.

Thus, from all these results, it can be concluded that the contact angle significantly increases with concentration on hydrophilic surfaces. The increase for the studied surfaces is at least on the order of 10° and can reach up to 35°. The results also indicate that care should be taken in preparing the samples (in particular regarding the cleaning procedure) in order to obtain reproducible results.

It is hard to conclude to any tendency for the hydrophobic glass surface, see Table 4. It seems that the contact angle is not significantly affected in this case. This is confirmed by the data for the glass coated with RTV-2 reported in Table 5, which show no significant variation of contact angle with concentration.

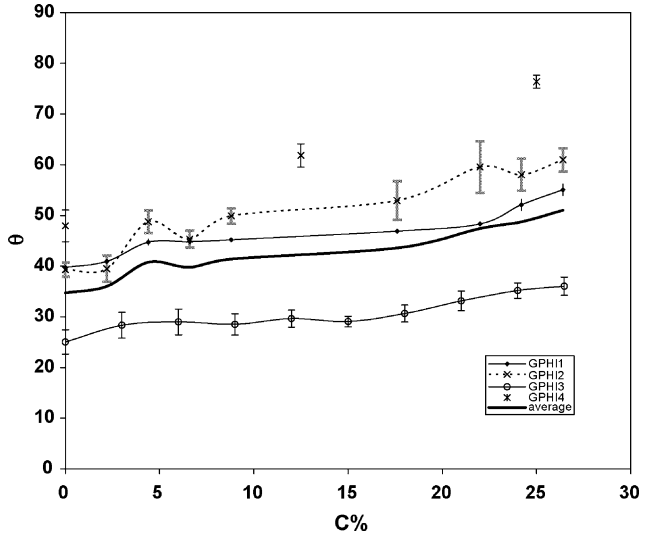

Fig. 2. Evolution of contact angle as a function of NaCl concentration for the hydrophilic glass samples. The thick solid line corresponds to the average over the whole set of data of series GPHI1, GPHI2 and GPHI3.

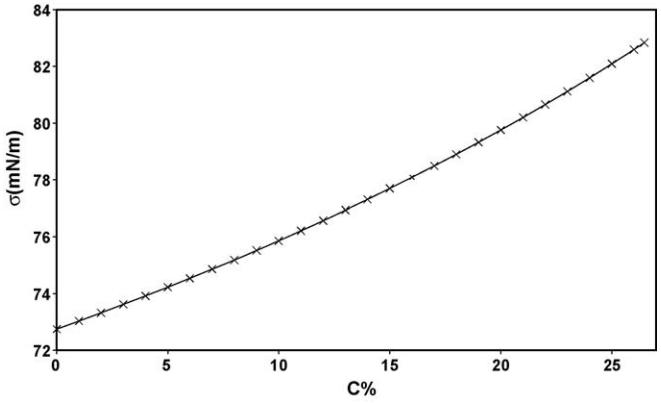

Fig. 3. Evolution of surface tension with C.

Although the physical origin of the contact angle variations remains to be investigated in details and could have to do with the adsorption of ions at the solid surface [10], our results indicates that a rough estimate of the contact angle variations can be deduced from the consideration of the contact line mechanical equilibrium, i.e. using the Young relation, e.g. [7,12], which reads

$$\sigma \cos\theta = \sigma_{sg} - \sigma_{sl} \quad (1)$$

where σ and σ_{sg} are the surface tensions of the liquid and solid, respectively, and σ_{sl} is the interfacial tension between the liquid and the solid. The surface tension σ (which is the interfacial tension between the liquid and the gas) is also a function of C, [11]. As depicted in Fig. 3, the surface tension σ increases with C. However, an interesting result emerges from Figs. 4 and 5 which show the evolution of $\sigma \cos\theta$ as a function of C for the glass surfaces and silicon wafers, respectively. Except for series GPHI4, the results shown in Figs. 4 and 5 indicate that the product $\sigma \cos\theta$ does not change appreciably with the concentration. From Eq. (1), this is an indication that the interfacial tension σ_{sl}

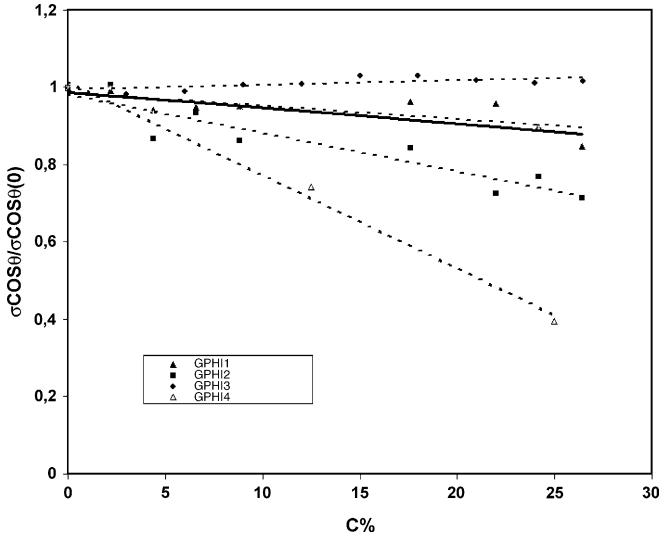

Fig. 4. Evolution of $\sigma \cos\theta/\sigma \cos(\theta)(0)$ as a function of C for glass. The dashed lines are least square fits of data for each series. The solid line is a least square fit of all the data of series GPHI1, GPHI2 and GPHI3.

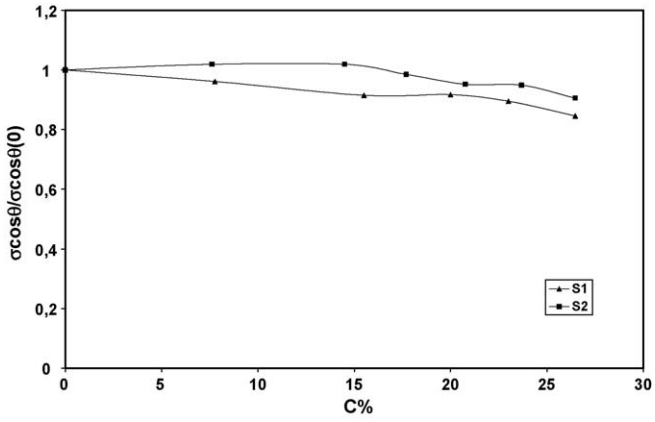

Fig. 5. Evolution of $\sigma \cos\theta$ as a function of C for the silicon wafers.

is not significantly affected by the presence of the salt and leads to the simple estimate of the contact angle variations with the salt concentration given by

$$\theta \approx \text{Arc cos}\left(\frac{\sigma(0)\cos\theta(0)}{\sigma(C)}\right) \quad (2)$$

where $\sigma(0)$ and $\theta(0)$ are the liquid surface tension and contact angle for pure water, respectively. As shown in Figs. 4 and 5 and Tables 1–5, Eq. (2) can be used as a rough estimate of the contact angle variations with the salt concentration. It is well known that the measured values lie between the values corresponding to the receding and advancing contact angles, the contact angle hysteresis introducing uncertainty in the measurement in addition to possible local change in wettability, e.g. [12]. Despite the measurement uncertainties, Eq. (2) clearly tends to underestimate the contact angle variations for the hydrophilic surfaces. The estimate given by Eq. (2) is consistent with the measurement uncertainties reported in Tables 3–5 when the contact angle for pure water is not very far from 90°. However, the variations of contact angle with the salt concentration are small in this case.

4. Discussion

In this section, we briefly discuss some possible impact of the contact angle variations on the physics and the modelling of ions transport in a porous medium. Two aspects are discussed, both related to capillary effects in porous media. The first one is the impact of contact angle variations on capillary pressure at the REV (representative elementary volume) scale as well as the pore scale. The second one is on the film flows associated with the thick liquid films that can take place in the corners or wedges of pore space.

We begin with a discussion of slow evaporation and quasi-static drainage in a hydrophilic material. As discussed in Ref. [8], slow evaporation in a hydrophilic material has some common features with quasi-static drainage. In particular, both situations can be simulated on pore-network models by using invasion percolation (IP) concepts. As it is well known, the IP algorithm is an algorithm of bond (throat) selection in which the bond of lowest capillary pressure threshold available on the liquid–gas interface is selected at each step of invasion. This capillary pressure threshold is of the form $P_c \approx \sigma \cos\theta/r$, where σ is the surface tension and θ the contact angle; r is a threshold average radius of curvature depending on the throat geometry (for a cylindrical throat of radius R, $r = R/2$). It is important to realize from the expression of P_c that this is in fact the product $\sigma \cos\theta$ rather than simply the contact angle that should be characterized as a function of C to explore the impact of the salt concentration variation on the invasion pattern. At a macroscopic scale, the macroscopic capillary pressure is an input data for the continuum models, e.g. [5]. Very often the macroscopic capillary pressure is expressed in terms of the Leverett J function as $P_c = \sigma \cos\theta\, J(S)/\sqrt{k/\varepsilon}$, where S is the water saturation, k the permeability and ε is the porosity of the porous medium, e.g. [12]. Again, the group $\sigma \cos\theta$ is the important factor to assess the impact of salt concentration on capillary equilibrium at REV scale.

As discussed before, our results indicate that the product $\sigma \cos\theta$ does not vary appreciably as a function of C. Thus we do not expect a major effect of spatial salt concentration variations on the invasion pattern. For completeness, we briefly discuss, however, the possible impact of a decrease of $\sigma \cos\theta$ with the concentration since such a decrease is consistent with some of the data reported in Figs. 4 and 5. When $\sigma \cos\theta$ decreases with concentration, the capillary pressure threshold P_c of a throat tends to be lower in a region of a high concentration compare to a throat of same size in a region of lower concentration. This opens up the possibility of an invasion percolation in a gradient effect associated with a gradient of concentration over the sample or owing to higher concentrations near the porous medium surface (as discussed for instance in Ref. [6], evaporation generally leads to higher concentration towards the porous medium surface owing to the convective transport in liquid phase induced by evaporation). By analogy with similar problems where the gradient of $\sigma \cos\theta$ is due to thermal gradients, e.g. [13], one expects a stabilizing effect, see Ref. [13] or [8] for more details. However, according to Figs. 4 and 5, the variations of $\sigma \cos\theta$ are at best of 20% if we discard the data close to the saturation concentration (because crystallisation would occur soon when such concentrations are reached and would affect the invasion pattern much more than the effect discussed here). Again by analogy with the results presented in Ref. [13], it is likely that the effect of $\sigma \cos\theta$ variation will be masked by viscous effects or only visible for unrealistically weakly disordered porous media, see Ref. [13] for details. Thus we conclude that variations of $\sigma \cos\theta$ of the order of the ones deduced from our data are not sufficient to significantly affect the evolution of the main features of liquid distribution during evaporation. However, this analysis ignores the effects of liquid wetting films.

As discussed in Refs. [14,15], liquid films can be trapped by capillarity in the corners of pore space when the bulk is invaded by the gas phase as a result of evaporation. This is illustrated in Fig. 6 for the idealized geometry of a pore of square cross-section. These films can be termed “thick” films in order to distinguish them from the very thin films of the order of nanometers that form when the liquid is perfectly wetting. Dynamics of thick films depends on capillary pressure (through the Young–Laplace equation), e.g. [16,17], whereas thin films depend on disjoining pressure. As shown in Refs. [14,15], the

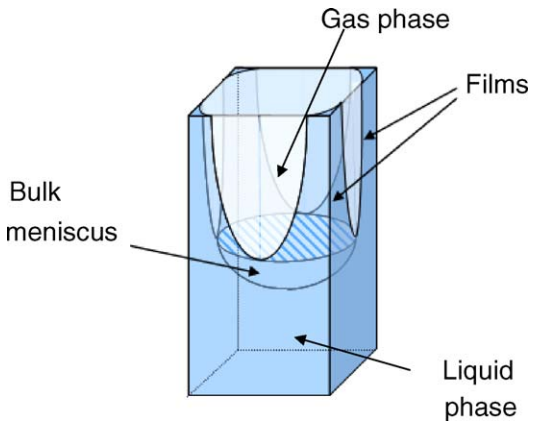

Fig. 6. Schematic of corner liquid films when the bulk of a pore is invaded by the gas phase.

presence of thick films greatly affects the evaporation rates since they offer a transport mechanism in liquid phase towards the porous medium surface that is much more efficient than water vapour diffusion in gas phase. Thick films also have an important influence on salt transport. According to the data presented in Ref. [18], the variation of the salt effective diffusion coefficient D_{eff} as a function of saturation is significantly affected by the transport in thick films. As mentioned before the evolution of salt distribution within the sample is directly dependent on the Peclet number, e.g. [6] for a situation where transport is induced by evaporation. The Peclet number is defined as $Pe = UL/D_{\text{eff}}$, where U is a characteristic liquid average velocity and L is the sample size. As D_{eff} varies with S, Pe varies during a process inducing saturation variations (drainage, infiltration, evaporation) and these variations depend on the way that D_{eff} varies with S, i.e. on the presence of thick films. For instance in the case of evaporation of a salt-water solution in a porous medium both the evaporation flux and the evolution of salt distribution are significantly affected by thick films through the impact of thick films on the position of evaporation front and effective coefficient D_{eff}. Clearly the impact of contact angle variations on thick films appears to be an important issue in the context of salt transport in unsaturated porous materials.

To get some insight into this issue, we consider two examples of idealized "pore": capillaries of square cross-section and capillaries of equilateral triangular cross-section. In passing, we note that these shapes are classically considered in pore-network models, e.g. [19,20]. The shape of gravity-free menisci in polygonal capillaries has been studied in detail in Ref. [21]. As discussed in Ref. [21], there exists a critical contact angle θ_c above which thick films cannot exist. Values of θ_c for three shapes of regular polygonal cross-section are given in Table 6. In addition some data on the maximum film thickness as a function of contact angle drawn from Ref. [21] are given in Table 7. The definition of maximum film thickness is given in Fig. 7.

Table 6
Critical contact angle θ_c in polygonal capillaries (from Ref. [20])

Polygon shape, N	θ_c (°)
3	60
4	45
6	30

N is the number of sides forming the cross-section. $N=3$ corresponds to an equilateral triangle, $N=4$ to a square (see Fig. 6), $N=6$ to a hexagon.

Table 7
Maximum film thickness δ as a function of contact angle in polygonal capillaries (from Ref. [20])

Polygon shape, N	θ (°)	δ/d
3	0	0.162
3	15	0.155
3	30	0.131
3	45	0.087
4	0	0.110
4	15	0.099
4	30	0.066
4	40	0.027

N is the number of sides forming the cross-section. $N=3$ corresponds to an equilateral triangle, $N=4$ to a square, d is the length of one side of polygon.

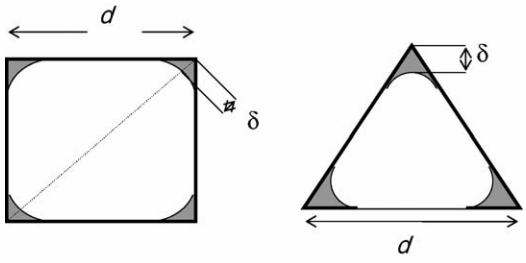

Fig. 7. Maximum film thickness δ.

As can be seen from the data of Tables 1, 2 and 6, it is possible that the films disappear during evaporation as the contact angle increases with concentration. For instance, this would happen for the three shapes of capillary with the data corresponding to GPHI1, GPHI2 and GPHI4 since the contact angle becomes higher than θ_c for sufficiently high salt concentration. This is also the case with the data corresponding to GPHI3 for the hexagonal shape. If the evolution of contact angle is similar to the one measured on the silicon wafers, the films would almost disappear if the pore shape can be assimilated to triangular cross-section. When the films are present, it can be noted that their thickness would greatly decrease as the concentration increases if our data apply to real porous media.

From the above analysis we conclude that contact angle variations with concentration can have a major effect on salt transport and evaporation in unsaturated soils or porous materials owing to the possible change in the hydraulic connectivity associated with thick films.

5. Conclusion

It has been found that the equilibrium contact angle varies with the salt concentration. As a rough estimate, these variations can be determined simply by using Eq. (2), which is deduced from the Young relation. Eq. (2) indicates significant contact angle variations with salt concentration when the contact angle for pure water is low, which is consistent with our measurements

for two types of hydrophilic surface: glass and silicon. Then we have discussed the possible consequences of such variations on salt transport in an unsaturated porous medium as well as evaporation in the presence of salt. The analysis indicates that the contact angle variations with concentration can have a major effect on salt transport and evaporation in unsaturated soils or porous materials owing to the possible change in the hydraulic connectivity associated with thick films.

However this conclusion is based on a set of data for artificial surfaces (as opposed to "real" porous materials such as stones, bricks, rocks or soils) and on the consideration of highly idealized "pore" geometries. Thus it would be desirable to study the effect of concentration variations on wettability and liquid film transport in real porous media in order to confirm our findings. Nevertheless, the main finding of this paper, i.e. the possible influence of contact angle variations with concentration on thick film hydraulic connectivity, should be kept in mind when analyzing experimental results of drying in the presence of salt or the salinisation problem evoked in the introduction.

Also, the influence of salt concentration on contact angle would deserve to be explored on other types of surface and with other salts.

Acknowledgements

We thank P. Abgral, P. Bachin, C. Marques, A.M. Gué, G. Lopez-Marti and N. Sakly for the help regarding the contact angle measurements and the silanization procedure and Professor R.R. Mazzoco for bringing the work of Gibanova et al. [10] to our attention. We also thank N. Bonn for valuable discussions.

References

[1] A. Goudie, H. Viles, Salt Weathering Hazards, Wiley, Chichester, 1997.
[2] P. Lal, B.R. Chhipa, A. Kumar, Salt affected soils and crop production: a modern synthesis, Reprint from: Jodhpur, Agrobios, 2003.
[3] T. Dracos, Multiphase flow in porous media, in: J. Bear, J.M. Buchlin (Eds.), Modelling and Applications of Transport Phenomena in Porous Media, Kluwer, 1991, pp. 195–220.
[4] R. Helmig, Multiphase Flow and Transport Processes in the Subsurface, Springer, 1997.
[5] O.A. Plumb, Transport phenomena in porous media: modeling the drying process, in: K. Vafai (Ed.), Handbook of Porous Media, Marcel Dekker, 2000, pp. 755–785.
[6] H.P. Huinink, L. Pel, M.A.J. Michels, How ions distribute in a drying porous medium: a simple model, Phys. Fluids 14 (4) (2002) 1389–1395.
[7] P.G. de Gennes, F. Brochard-Wyart, D. Quéré, Gouttes, bulles, perles et ondes, Belin, 2002.
[8] M. Prat, Recent advances in pore-scale models for drying of porous media, Chem. Eng. J. 86 (1/2) (2002) 153–164.
[9] P. Van Der Voort, E.F. Vansant, Silylation of the silica surface: a review, J. Liq. Chromatogr. Rel. Technol. 19 (1996) 2723–2752.
[10] E.V. Gibanova, E.V. Mashonskaya, L.M. Cherkashina, Effect of solution concentration on quartz contact angles, Translated from Kolloidnyi Zhurnal 50 (4) (1988) 818–821.
[11] Robert C. Weast (Ed.), Handbook of Chemistry and Physics, Edition 1980–1981, CRC Press, 1981.
[12] F.A.L. Dullien, Porous Media, Fluid Transport and Pore Structure, Academic Press, 1991.
[13] F. Plourde, M. Prat, Pore network simulations of drying of capillary media. Influence of thermal gradients, Int. J. Heat Mass Tr. 46 (2003) 1293-L1307.
[14] J.B. Laurindo, M. Prat, Numerical and experimental network study of evaporation in capillary porous media. Drying rates, Chem. Eng. Sci. 53 (12) (1998) 2257–2269.
[15] A.G. Yiotis, A.G. Boudouvis, A.K. Stubos, I.N. Tsimpanogiannis, Y.C. Yortsos, The effect of liquid films on the drying of porous media, AIChE J. 50 (11) (2004) 2721–2737.
[16] B. Camassel, N. Sghaier, M. Prat, S. Ben Nasrallah, Ions transport during evaporation in capillary tubes of polygonal cross section, Chem. Eng. Sci. 60 (2005) 815–826.
[17] T. Coquard, B. Cammassel, M. Prat, Evaporation in capillary tubes of square cross section, in: Proceedings of HT2005, 2005 Summer ASME Heat Transfer Conference, San Fancisco, CA, USA, July 17–22, 2005.
[18] S.L. Barbour, The soil–water characteristic curve: a historical perspective, Can. J. Geotech. J. 35 (1998) 873–894.
[19] Y. Le Bray, M. Prat, Three dimensional pore network simulation of drying in capillary porous media, Int. J. Heat Mass Tr. 42 (1999) 4207–4224.
[20] M.J. Blunt, M.D. Jackson, M. Piri, P.H. Valance, Detailed physics, predictive capabilities and macroscopic consequences for pore-network models of multiphase flow, Adv. Water Res. 25 (2002) 1069–1089.
[21] H. Wong, S. Morris, C.J. Radke, Three dimensional menisci in polygonal capillaries, J. Colloids Interf. Sci. 148 (2) (1992) 317–336.